JPET Fast Forward. Published on July 7, 2006 as DOI: 10.1124/jpet.106.108399

JPET #108399

Identification and Characterization of Functional Rat Arylamine N-acetyltransferase 3: Comparisons with Rat Arylamine N-acetyltransferases 1 and 2

Jason M. Walraven, Mark A. Doll, and David W. Hein

Department of Pharmacology & Toxicology and James Graham Brown Cancer Center,

University of Louisville School of Medicine, Louisville, KY

a) Characterization of rat N-acetyltransferases 1, 2, and 3

b) Corresponding author: David W. Hein, Ph.D., Department of Pharmacology and Toxicology, University of Louisville School of Medicine, Louisville, KY 40292, Phone: (502) 852-5141; Fax: (502) 852-7868; Email: d.hein@louisville.edu

c) The number of text pages: 25
The number of tables: 3
The number of figures: 4
The number of references: 37
The number of words in the Abstract: 216
The number of words in the Introduction: 797
The number of words in the Discussion: 1026

d) Non-standard Abbreviations Used in this Paper:

Human N-acetyltransferase 1 (NAT1), human N-acetyltransferase 2 (NAT2), rat or mouse N-acetyltransferase 1 (Nat1); rat or mouse N-acetyltransferase 2 (Nat2); rat or mouse N-acetyltransferase 3 (Nat3), human N-acetyltransferase pseudogene (NATP); open reading frame (ORF), Fisher 344 (F344), Sprague Dawley (SPRD), Wistar Kyoto (WKY), 3-ethylaniline (3EA), 3,5-dimethylaniline (35DMA), o-toluidine (OT), 2,6-dimethylaniline (26DMA), 5-aminosalicylic acid (5AS), p-aminobenzoic acid (PABA), p-aminoacetanilide (PAA), 3-amino-4-methoxyacetanilide (3A4MAA), N-(p-aminobenzoyl)glutamate (pABG), procainamide (PA), 4-aminobiphenyl (ABP), 4,4'-methylenedianiline (MDA), 4,4'-methylenebis(2-chloroaniline) (MOCA), 2-aminofluorene (AF), isoniazid (INH), sulfamethazine (SMZ), N-hydroxy-4-aminobiphenyl (N-OH-ABP)

e) Recommended section assignment:

Toxicology, Cellular and Molecular

ABSTRACT

Arylamine N-acetyltransferases (NAT; EC 2.3.1.5) catalyze both the N-acetylation and O-acetylation of arylamines and hydrazines. Humans possess two functional N-acetyltransferase genes, *NAT1* and *NAT2*, as well as a non-functional pseudogene, *NATP*. Previous studies have identified *Nat1* and *Nat2* genes in the rat. In this study, we identified and characterized a third rat N-acetyltransferase gene (*Nat3*) consisting of a single open reading frame of 870 base pairs encoding a 290 amino acid protein, analogous to the previously identified human and rat N-acetyltransferase genes. Rat *Nat3* nucleotide sequence was 77.2% and 75.9% identical to human *NAT1* and *NAT2*, respectively. Rat Nat3 amino acid sequence was 68.6% and 67.2% identical to human NAT1 and NAT2, respectively. Rat *Nat1*, *Nat2*, and *Nat3* were each cloned and recombinantly expressed in *Escherichia coli*. Recombinant rat Nat3 exhibited thermostability intermediate between recombinant rat Nat1 and Nat2. Recombinant rat Nat3 was functional and catalyzed the N-acetylation of several arylamine substrates, including 3-ethylaniline, 3,5-dimethylaniline, 5-aminosalicylic acid, 4-aminobiphenyl, 4,4'-methylenedianiline, 4,4'-methylenebis(2-chloroaniline), and 2-aminofluorene, and the O-acetylation of N-hydroxy-4-aminobiphenyl. The relative affinities of arylamine carcinogens such as 4-aminobiphenyl, N-hydroxy-4-aminobiphenyl, and 2-aminofluorene for N- and O-acetylation via recombinant rat Nat3 were comparable to recombinant rat Nat1 and higher than for recombinant rat Nat2. This study is the first to report a third arylamine N-acetyltransferase isozyme with significant functional capacity.

INTRODUCTION

Arylamine N-acetyltransferases (NAT; EC 2.3.1.5) catalyze acetyl group transfer from acetyl-coenzyme A, or another acetyl donor, to the exocyclic amine of arylamines (N-acetylation) or the hydroxyl oxygen of N-hydroxylated arylamines (O-acetylation) (Hein, 1988). N-acetyltransferases can bioactivate (O-acetylation) or deactivate (N-acetylation) arylamine pro-carcinogens such as 4-aminobiphenyl, a component of cigarette smoke (Patrianakos et al., 1979). NATs also metabolize various pharmaceutical drugs such as the antitubercular drug isoniazid, antibacterial sulfonamides, and the antiarrhythmic procainamide (Evans et al., 1960; Parker, 1969; Weber and Hein, 1985). Further insight into N-acetyltransferase function, expression, and regulation may predict individual incidences of pharmaceutical drug toxicities or individual tissue-specific cancer susceptibilities associated with environmental and/or occupational arylamine pro-carcinogen exposures.

The human genome contains two functional arylamine N-acetyltransferase loci, *NAT1* and *NAT2*, coding for arylamine N-acetyltransferase enzymes that can be distinguished on the basis of substrate selectivity, structural stability, tissue-specific expression profile, and kinetic activity toward arylamine substrates (Blum et al., 1990; Hein et al, 1993; Boukouvala and Fakis, 2005). Humans also possess a non-functional pseudogene, *NATP* (Blum et al., 1990).

Rat models have been utilized for the study of arylamine N-acetyltransferases (Wick and Hanna, 1990; Hein et al., 1991; Hein et al., 1997; Grundmann et al., 2004; Lin et al., 2005; Zhang et al., 2006). Rat arylamine N-acetyltransferases are very similar in sequence and function to human N-acetyltransferases (Hein et al., 1997). Residues 125, 127, and 129 of the 290 amino acid protein determine substrate access to the active site, thereby influencing substrate

selectivity (Goodfellow et al., 2000). Rat Nat2 and human NAT1 amino acid sequences both contain Phe125, Arg127, Tyr129, which is predictive of their similar arylamine substrate selectivities. On the other hand, the human NAT2 protein contains Ser125, Ser127, Ser129 and the rat Nat1 protein contains Tyr125, Ser127, Tyr129, which is predictive of a weaker correlation between rat Nat1 and human NAT2 arylamine substrate selectivities. The same relationship is observed with regard to acetyl-donor substrate selectivities. The C-terminal undecapeptide, which is involved in controlling acetyl-coenzyme A hydrolysis (Mushtaq et al., 2002), is 100% identical when comparing rat Nat2 and human NAT1, but only 54 % identical when comparing rat Nat1 and human NAT2. In terms of structural stability, human NAT2 is a more stable enzyme than human NAT1, and rat Nat1 is a more stable enzyme than rat Nat2, possibly suggesting structural similarities between the stable rat Nat1 and human NAT2, and the relatively unstable rat Nat2 and human NAT1 (Hein et al., 1993; Hein et al., 1997).

Identification of a third mouse *Nat* locus by Kelly and Sim (1994) suggested a third *Nat* locus in rodents. Land et al. (1996) published southern blot analyses for rat *Nat1* and *Nat2* that suggested the presence of a third rat N-acetyltransferase gene. Recently, a "*rattus norvegicus* similar to mouse *Nat3*" (original title) open reading frame (ORF) sequence (XM_224762) was predicted by automated computational analysis of annotated genomic sequence NW_047470 using gene prediction method GNOMON (National Center for Biotechnology Information). The genomic sequence for this entry originated from rat strain BN/SsNHsd/MCW. According to NCBI Map Viewer (Wheeler et al., 2005) and BLAT from UCSC Genome Bioinformatics (Kent, 2002), the rat Nats are located within about 75 kb and map to 16p14 on rat chromosome 16. The order of the rat Nat genes on chromosome 16 from 5' to 3' is *Nat1-Nat2-Nat3*, from centromere to telomere, with about 10 kb between *Nat1* and *Nat2*, and about 60 kb between *Nat2* and *Nat3*.

This is similar to the arrangement of mouse *Nat3* relative to mouse *Nat1* and *Nat2* on mouse chromosome 8 (Boukouvala and Fakis, 2005). However, mouse Nat3 has extremely low catalytic activity, and N-acetylated only a few arylamine substrates (Estrada-Rodgers et al., 1998; Fretland et al., 1997). Since the predicted rat *Nat3* gene is highly homologous to mouse *Nat3* in both nucleotide and predicted amino acid sequence, 91.0% and 87.9% identical, respectively, rat Nat3 may also have very low activity compared to rat Nat1 and Nat2.

The rat *Nat3* ORF from GenBank entry XM_224762 was predicted from a large scale genome project, and could contain sequencing errors. In addition, since the Brown Norway inbred rat strain is genetically closer to wild rats than it is to other inbred rat strains, the predicted sequence may not be identical to the *Nat3* ORF found in other common inbred rat strains (Canzian, 1997; Thomas et al., 2003). The aims of this study included complete sequencing of the putative rat *Nat3* gene from three inbred rat strains, cloning the putative rat *Nat3* ORF into a prokaryotic expression vector, and recombinant expression of the rat *Nat3* gene in a high expressing bacterial system to characterize Nat3 catalytic activity, substrate selectivity, and intrinsic stability. Rat Nat1 and Nat2 were also analyzed in the same system in parallel for comparison to rat Nat3.

METHODS

Cloning and Sequencing

Rat *Nat1* and *Nat2* were cloned into pKK223-3 prokaryotic expression vector as previously described (Doll and Hein, 1995). The 870 base pair *Nat3* ORF was amplified from Fisher 344 (F344), Sprague Dawley (SPRD), and Wistar Kyoto (WKY) genomic DNA by duplicate independent PCR reactions. As a control, these duplicate PCR reactions were carried through the following cloning and sequencing steps in parallel. Gene-specific *Nat3* PCR primers (Table 1) were designed based on the predicted *Nat3* sequence from GenBank accession number XM_224762 with restriction sites *XmaI* and *PstI* designed into the primer to facilitate directional cloning into the expression vector. The *Nat3* ORF was cloned into pcDNA3.1 vector by TA cloning (Invitrogen, Carlsbad, CA), and the *Nat3* ORF insert was completely sequenced (top and bottom strands) using commercially available pcDNA3.1 specific primers T7 (forward) and BGH (reverse) (Invitrogen), and six *Nat3* specific forward and reverse primers (Table 1). Sequencing reactions were performed using BigDye Terminator v1.1 Cycle Sequencing Kit (Applied Biosystems, Foster City, CA, USA), and analyzed with an ABI Prism 310 Genetic Analyzer (Applied Biosystems). Sequencing data was aligned to verify sequence using SeqMan II version 5.03 from DNASTAR Inc. (Madison, WI).

Sub-cloning and Expression

The rat *Nat3* ORF insert was subcloned into the pKK223-3 bacterial expression vector (Pharmacia-LKB Biotechnology, Piscataway, NJ) in duplicate using *XmaI* and *PstI* restriction enzymes. Duplicate clones were carried through the expression steps as a control. The 5’ and 3’

ligation sites were verified by sequencing. JM105 strain *Escherichia coli* were made competent and transformed with the *Nat3*/pKK223-3 plasmid using previously described methods (Chung and Miller, 1988; Chung et al, 1989). JM105 competent *Escherichia coli* were transformed with an empty pKK223-3 vector as a negative control.

Recombinant *Nat1*, *Nat2*, *Nat3*, and vector were expressed in JM105 *Escherichia coli* as previously described (Doll and Hein, 1995). Total bacterial lysate protein concentration was determined for each expression (Bradford, 1976).

Western Blotting

A 19-residue peptide (N-VLKRVFGIRLETKLVPKCGNWLFTI-C) was designed for Nat3-selective polyclonal antiserum production. The peptide matches C-terminal residues 266–290 of the deduced rat Nat3 amino acid sequence, and differs from the same regions of rat Nat1 and Nat2 by nine residues and ten residues, respectively. Peptide synthesis and polyclonal antiserum production were accomplished by Invitrogen.

Bacterial lysates were diluted to 1 mg/ml in homogenization buffer (20 mM sodium phosphate, 1 mM ethylenediaminetetraacetic acid, 1mM dithiothreitol, protease inhibitor cocktail, pH 7.4) and Laemmli loading buffer (5% 2-mercaptoethanol) (BioRad), boiled for 5 minutes, electrophoresed through 12% Tris/Glycine PAGEr Duramide Gels (Cambrex, East Rutherford, NJ) in 1x Tris/Glycine/SDS running buffer (BioRad), and transferred to Amersham Hybond-ECL nitrocellulose membrane with a TE 70 Semi-Dry Transfer Unit (GE Healthcare) in 1x Tris/Glycine transfer buffer (BioRad). The membrane was stained with Ponceau S solution to verify equal protein loading. After stain removal, membranes were blocked overnight at 4ºC with Blocker Blotto in TBS (Pierce Biotechnology, Rockford, Il), then incubated with primary

antiserum in blocking buffer plus 0.05% Tween-20 at room temperature for 2 hr, and with goat anti-rabbit horseradish peroxidase-conjugated secondary antibody in blocking buffer plus 0.05% Tween-20 at RT for 1 hr. Tris-buffered saline washing steps (3 x 10 min) were included between the primary and secondary antibody incubations and after the secondary antibody incubation. Membranes were incubated with Amersham ECL Plus chemiluminescent working solution (GE Healthcare), exposed to Kodak Bio-Max film, and developed using a Kodak X-OMAT 2000A processor.

Enzyme Activity Assays

Bacterial lysates expressing recombinant *Nat1*, *Nat2*, *Nat3* or vector (negative control) were assayed for N-acetylation of 3-ethylaniline (3EA), 3,5-dimethylaniline (35DMA), o-toluidine (OT), 2,6-dimethylaniline (26DMA), 5-aminosalicylic acid (5AS), p-aminobenzoic acid (PABA), p-aminoacetanilide (PAA), 3-amino-4-methoxyacetanilide (3A4MAA), N-(p-aminobenzoyl)glutamate (pABG), procainamide (PA), 4-aminobiphenyl (ABP), 4,4'-methylenedianiline (MDA), 4,4'-methylenebis(2-chloroaniline) (MOCA), 2-aminofluorene (AF), isoniazid (INH), and sulfamethazine (SMZ), and for O-acetylation of N-hydroxy-4-aminobiphenyl (N-OH-ABP).

Bacterial lysates were assayed for N-acetylation of PABA, pABG, ABP, AF, SMZ, MDA, and MOCA by measurement of N-acetylated product. For initial velocity measurements, lysates (in triplicate) were incubated with 1 mM acetyl-coenzyme A and 300 μM substrate (100 μM MDA or MOCA) for 10 minutes at 37ºC, and the reaction stopped upon addition of 1/10 volume of 1 M acetic acid. Control reactions substituted water for acetyl-coenzyme A. N-acetylated products were separated and measured using a Beckman System Gold high performance liquid

chromatography (HPLC) system. HPLC methods for measuring the N-acetylation of PABA, ABP, AF, SMZ, and MDA have been previously described (Leff et al., 1999; Fretland et al., 2002; Zhang et al, 2006). The HPLC separation for the N-acetylation of MOCA was identical to the MDA method, with mono-acetyl-MOCA eluting at 16.5 min. pABG and N-acetyl-pABG product were separated by HPLC with a mobile phase of 20 mM sodium perchlorate (pH 2.5) and acetonitrile. Elution was conducted with a linear gradient from 0% acetonitrile / 100% sodium perchlorate to 50% acetonitrile / 50% sodium perchlorate over 5 min at a flow rate of 2 ml/min. Under these conditions, N-acetyl-pABG eluted at 9.5 min.

Bacterial lysates were assayed for N-acetylation of PAA, 3EA, 35DMA, OT, 26DMA, 3A4MAA, INH, PA, and 5ASA as above, then analyzed using a colorimetric assay as previously described (De Angelis et al., 1998). Briefly, to a 300 μL reaction, 600 μL of 3.2 M guanidine HCl / 0.1 M sodium phosphate (pH 6.8) and 0.1 ml of 2 mM 5,5'-dithio-bis(2-nitrobenzoic acid (DTNB) / 0.1 M sodium phosphate (pH 6.8) / 10 mM EDTA were added and incubated at room temperature for 5 minutes. Controls substituted water for substrate. Bacterial lysates (diluted to 3 mg/ml in homogenization buffer) were assayed for O-acetylation of N-OH-ABP by HPLC separation and measurement of ABP-deoxyguanosine adduct as previously described (Hein et al., 2006).

For determinations of apparent Michaelis-Menten kinetic parameters K_m (μM) and V_{max} (nmoles/min/mg), initial velocities were determined using a range of substrate concentrations. The data were fitted to a one-phase exponential association non-linear regression curve using GraphPad Prism V2.01 software (GraphPad Software, Inc., San Diego, CA). A specificity constant was calculated (V_{max}/K_m) which, assuming equal Nat1, Nat2, and Nat3 protein expression, could approximate the rate of substrate capture (Fersht, 1998).

Thermostability

Bacterial lysates diluted to 1 mg/ml in homogenization buffer were incubated at either 37ºC or 50ºC for 5, 10, 20, 40, 60, or 80 minutes, transferred immediately to ice, and assayed for N-acetylation of AF. Results were normalized to activity of un-incubated enzyme (time zero = 100%) for the percent activity remaining. Heat inactivation half-life ($T_{½}$) and heat deactivation constant (k) were determined by fitting the data to a first-order decay curve using GraphPad Prism software.

RESULTS

Cloning and Sequencing Rat Nat3

The *Nat3* ORF in inbred strains F344, WKY, and SPRD were identical (GenBank accession numbers AY253757, AY253758, and AY253759). The *Nat3* ORF in these rat strains differed from the predicted *Nat3* ORF, XM_224762, from rat strain Brown Norway (BN), at ORF nucleotide 358.

Recombinant expression of rat Nat3

Western blotting with rat Nat3 antiserum selectively detected the presence of recombinant Nat3 enzyme in bacterial lysates derived from *Escherichia coli* transformed with rat *Nat3*. In contrast, an N-acetyltransferase band was not visible in bacterial lysates derived from *Escherichia coli* transformed with rat *Nat1*, *Nat2*, or vector (Figure 2). Ponceau S staining confirmed equal total protein loading in each lane. Due to differences in immunoreactivity of the antibodies used to detect each isozyme, and the indistinguishable size of the Nat band in total protein stain, the amount of recombinant protein in each lysate could not be compared.

Recombinant Rat N-acetyltransferase Activity

N-acetylation activity of recombinant rat Nat1, Nat2, and Nat3 for thirteen substrates is summarized in Figure 3. Recombinant rat Nat3 N-acetylated ABP, AF, MDA MOCA, 35DMA, 3EA, and 5AS, but not INH, PA, PABA, SMZ, pABG, PAA, or 3EA. Recombinant rat Nat1 N-acetylated all substrates except pABG. Recombinant rat Nat2 N-acetylated all substrates except INH. Recombinant rat Nat1, Nat2, and Nat3 each catalyzed the O-acetylation of N-OH-ABP

(Table 2). No N-acetylation activity was detected towards OT, 26DMA, or 3A4MAA for any rat N-acetyltransferase. Background activity was extremely low or undetectable for all substrates tested.

Apparent Michaelis-Menten Kinetics

Recombinant rat Nat2 had the highest apparent V_{max} and K_m for the N-acetylation of ABP and AF, and for the O-acetylation of N-OH-ABP (Table 2). Although recombinant rat Nat2 had the lowest affinity for these substrates, it catalyzed their N-acetylation and O-acetylation at much higher rates than recombinant Nat1 or Nat3. For each of these substrates, recombinant rat Nat1 and Nat3 apparent K_m values were comparable, indicating similar affinities for the substrates, though recombinant Nat3 had a lower apparent V_{max}, and therefore the slowest reaction velocity relative to recombinant rat Nat1 and Nat2. O-acetylation activity was detected for all three recombinant isozymes at much lower rates than for N-acetylation (lower V_{max}). Also, recombinant rat Nat1, Nat2, and Nat3 affinity for the N-hydroxylated substrate N-OH-ABP was much lower (higher K_m) in comparison to AF or ABP.

Thermostability

Lysates were assayed at 37ºC and 50ºC, as described in methods, however, thermostability differences among the recombinant rat Nat isozymes were most readily observed at 50ºC (Figure 4). Recombinant Nat1 was the most stable with no reduction in activity after 120 minutes incubation at 50ºC (data only shown to 80 min). Recombinant Nat3 lost most of its activity following 80 minutes of incubation, and was less stable than recombinant Nat1, but more stable than recombinant Nat2. Recombinant Nat2 was relatively unstable, having lost most of its

activity within 5 minutes of incubation at 50ºC.

DISCUSSION

Cloning and sequencing of rat Nat3 from rat genomic DNA, and recombinant expression of rat Nat1, Nat2, and Nat3 in parallel provided an opportunity to characterize rat Nat3 in comparison with rat Nat1 and Nat2. This study identifies a rat *Nat3* ORF encoding for a functional arylamine N-acetyltransferase enzyme with intermediate intrinsic stability relative to rat Nat1 and Nat2 and that catalyes both N-acetylation and O-acetylation reactions. Multiple studies in bacterial and mammalian expression systems have reported very low to undetectable mouse Nat3 activity towards a limited number of substrates (Estrada-Rodgers et al., 1998; Fretland et al., 1997; Kelly and Sim, 1994). Recombinant rat Nat3 had low activity relative to recombinant Nat1 and Nat2, but future studies of *Nat1*, *Nat2*, and *Nat3* mRNA and protein expression in rat tissues are necessary to determine the relative contribution of rat Nat3 to acetylator phenotype in the rat.

Seven arylamine substrates were N-acetylated by recombinant rat Nat3, including ABP, AF, 5AS, 35DMA, 3EA, MDA and MOCA, although each of these substrates were also N-acetylated at higher rates by recombinant rat Nat1 and Nat2. In contrast, recombinant rat Nat1 selectively N-acetylated INH, MOCA, and PA, while recombinant rat Nat2 selectively N-acetylated PAA, PABA, pABG, ABP, AF, 5AS, 35DMA, 3EA, and MDA (Figure 3). Substrates PABA and SMZ are classic human NAT1 and NAT2 selective substrates, respectively (Grant et al., 1991). Recombinant rat Nat2 PABA selectivity is analogous to human NAT1. Although acetylated at relatively low rates by recombinant Nat1 and Nat2, SMZ was not selective for either recombinant rat Nat1 or Nat2, which may be attributed to additional steric interference at the rat Nat1 active site from larger tyrosine residues at 125 and 129 instead of the smaller human

NAT2 serine residues at 125 and 127 (Table 3).

Kawamura et al. (2005) describes a similar analysis of the substrate selectivities of purified human NAT1 and NAT2, and hamster Nat2, highlighting the similarities between hamster Nat2 and human NAT1. The results of that study of purified N-acetyltransferse enzymes agrees with this study of unpurified, recombinantly expressed rat N-acetyltransferases, thereby confirming both the result and expression system used in this study. Both studies measure activities for PABA, pABG, AF, INH, and PA, and found relative substrate selectivities that support the homologous relationship of human NAT1 to rat Nat2 and of human NAT2 to rat Nat1. The Kawamura et al. (2005) study likewise noted the similar substrate selectivity between human NAT1 and the rodent, in that case hamster, Nat2.

Recombinant rat Nat1, Nat2, and Nat3 differed in N-acetylation and O-acetylation reaction rates. Recombinant rat Nat2 catalyzed N-acetylation and O-acetylation at much higher rates than Nat1 or Nat3, regardless of substrate; however, these results were obtained by recombinant expression in a bacterial system. Since rats do not utilize the same degradation mechanisms as bacteria, expression in a mammalian system will be necessary to understand the influence of eukaryotic cell degradation mechanisms on the expression of rat Nat enzymes. Investigations into the expression of these arylamine N-acetyltransferases in mammalian cell culture and in rat tissues are in progress.

Rat *Nat3* consisted of a single open reading frame of 870 base pairs encoding a 290 amino acid protein, analogous to the previously identified human and rat N-acetyltransferase genes. Rat *Nat3* nucleotide sequence was 77.2% and 75.9% identical to human *NAT1* and *NAT2,* respectively. Rat Nat3 amino acid sequence was 68.6% and 67.2% identical to human NAT1 and NAT2, respectively (Figure 1). Whereas the predicted *Nat3* ORF from the BN rat strain has

JPET Fast Forward. Published on July 7, 2006 as DOI: 10.1124/jpet.106.108399
This article has not been copyedited and formatted. The final version may differ from this version.

a guanine (G) at nucleotide 358, the inbred rat strains F344, WKY, and SPRD rats had an adenine (A) at 358. The change A358>G results in a valine to isoleucine change at residue 120. However, mammalian N-acetyltransferase genes from human, rhesus monkey (Macaca mulatta), chimpanzee (Pan troglodytes), cattle (Bos taurus), cat (Felis catus), rabbit (Oryctolagus cuniculus), chinese hamster (Cricetulus griseus), golden hamster (Mesocricetus auratus), mouse (Mus musculus), and chicken (Gallus gallus) have an adenine at nucleotide position 358.

The Cys68, His107, Asp122 catalytic triad is present in rat *Nat3*, analogous to other mammalian Nats. The three residues (125, 127, 129) known to influence N-acetyltransferase substrate selectivity (Goodfellow et al., 2000) are unique to rat Nat3 among the human NATs and rat Nats, but identical to those found in the mouse *Nat3* sequence (Table 3), suggesting that Nat3 arylamine substrate selectivity is similar to mouse Nat3. The rat Nat3 C-terminal undecapeptide is 81.8% identical to mouse Nat3, 63.6% identical to human NAT1 and both rat Nat1 and Nat2, and 54.5% identical to human NAT2 (Table 3). Rat *Nat3* nucleotide sequence is 75.7% identical to rat *Nat1* and 78.0% identical to rat *Nat2*; rat Nat3 amino acid sequence is 71.0% identical to rat Nat1 and 71.7% identical to rat Nat2 (Figure 1). Rat Nat3 amino acid and nucleotide sequences are most identical to those of mouse Nat3, at 87.9% and 91.0%, respectively. The rat Nat3 catalytic core (63-131) (Rodrigues-Lima et al., 2001) is 72.5% identical to rat Nat1 and Nat2 catalytic cores, 73.9% identical to mouse Nat1 and Nat2 catalytic cores, and 89.9% identical to mouse Nat3 catalytic core. The rat *Nat3* nucleotide sequence is 70.3% identical to the sequence of the human *NAT* pseudogene (*NATP*), which is lower than the sequence identity of *NATP* with human *NAT1* and *NAT2*, and rat *Nat1* and *Nat2*. This low sequence identity combined with the difference in chromosomal orientation to the other two Nats (*NATP* is located between *NAT1* and *NAT2*) strongly suggests that human *NATP* and rat *Nat3* are

not homologous.

In summary, recombinant rat Nat3 was functional and catalyzed the N-acetylation of several arylamine substrates, including 3-ethylaniline, 3,5-dimethylaniline, 5-aminosalicylic acid, 4-aminobiphenyl, 4,4'-methylenedianiline, 4,4'-methylenebis(2-chloroaniline), and 2-aminofluorene, and the O-acetylation of N-hydroxy-4-aminobiphenyl. The relative affinities of arylamine carcinogens such as 4-aminobiphenyl, N-hydroxy-4-aminobiphenyl, and 2-aminofluorene for recombinant rat Nat3 were comparable to recombinant rat Nat1 and higher than for recombinant rat Nat2. This study is the first to report a third arylamine N-acetyltransferase isozyme with significant functional capacity. Future studies will involve characterization of recombinant rat N-acetyltransferases in mammalian cell systems, and utilization of the rat as an animal model for investigation of N-acetyltransferase activity, expression, and regulation *in vivo*.

REFERENCES

Blum M, Grant DM, McBride W, Heim M and Meyer UA (1990) Human arylamine N-acetyltransferase genes: isolation, chromosomal localization, and functional expression. *DNA Cell Biol* **9**:193-203.

Boukouvala S and Fakis G (2005) Arylamine N-acetyltransferases: what we learn from genes and genomes. *Drug Metab Rev* **37**:511-564.

Bradford MM (1976) A rapid and sensitive method for the quantitation of microgram quantities of protein utilizing the principle of protein-dye binding. *Anal Biochem* **72**:248-254.

Canzian F (1997) Phylogenetics of the laboratory rat Rattus norvegicus. *Genome Res* **7**:262-267.

Chung CT and Miller RH (1988) A rapid and convenient method for the preparation and storage of competent bacterial cells. *Nucleic Acids Res* **16**:3580.

Chung CT, Niemela SL and Miller RH (1989) One-step preparation of competent Escherichia coli: transformation and storage of bacterial cells in the same solution. *Proc Natl Sci USA* **86**:2172-2175.

De Angelis J, Gastel J, Klein DC and Cole, PA (1998) Kinetic analysis of the catalytic mechanism of serotonin N-acetyltransferase (EC 2.3.1.87). *J Biol Chem* **273**:3045-3050.

Doll MA and Hein DW (1995) Cloning, sequencing and expression of NAT1 and NAT2 encoding genes from rapid and slow acetylator inbred rats. *Pharmacogenetics* **5**:247-251.

Estrada-Rodgers L, Levy GN and Weber WW (1998) Substrate selectivity of mouse N-acetyltransferases 1,2, and 3 expressed in COS-1 cells. *Drug Metab Dispos* **26**:502-505.

Evans DAP, Manley KA and Mckusick VA (1960) Genetic control of isoniazid metabolism in man. *Br Med J* **2**:485-491.

Fersht AR (1998) *Structure and Mechanism in Protein Science: A Guide to Enzyme Catalysis and Protein Folding*. Freeman, New York.

Fretland AJ, Doll MA, Gray K, Feng Y and Hein DW (1997) Cloning, sequencing, and recombinant expression of NAT1, NAT2, and NAT3 derived from the C3H/HeJ (Rapid) and A/HeJ (Slow) acetylator inbred mouse: functional characterization of the activation and deactivation of aromatic amine carcinogens. *Toxicol Appl Pharmacol* **142**:360-366.

Fretland AJ, Doll MA, Zhu Y, Smith L, Leff MA and Hein DW (2002) Effect of nucleotide substitutions in N-acetyltransferase-1 on N-acetylation (deactivation) and O-acetylation (activation) of arylamine carcinogens: implications for cancer predisposition. *Cancer Detect Prev* **26**:10-14.

Goodfellow GH, Dupret J and Grant DM (2000) Identification of amino acids imparting acceptor substrate selectivity to human arylamine acetyltransferases NAT1 and NAT2. *Biochem J* **348**:159-166.

Grant DM, Blum M, Beer M and Meyer UA (1991) Monomorphic and polymorphic human arylamine N-acetyltransferases: a comparison of liver isozymes and expressed products of two cloned genes. *Mol Pharmacol* **39**:184-191.

Grundmann M, Earl CD, Sautter J, Henze C, Oertel WH and Bandmann O (2004) Slow N-acetyltransferase 2 leads to enhanced intrastriatal dopamine depletion in 6-hydroxydopamine-lesioned rats. *Exp Neurol* **187**:199-202.

Hein DW (1988) Acetylator genotype and arylamine-induced carcinogenesis. *Biochim Biophys Acta* **948**:37-66.

Hein DW, Rustan TD, Bucher KD, Furman EJ and Martin WJ (1991) Extrahepatic expression of the N-acetylation polymorphism towards arylamine carcinogenesis in tumor target organs of an inbred rat model. *J Pharmacol Exp Ther* **258**:232-236.

Hein DW, Doll MA, Rustan TD, Gray K, Feng Y, Ferguson RJ and Grant DM (1993) Metabolic activation and deactivation of arylamine carcinogens by recombinant human NAT1 and polymorphic NAT2 acetyltransferases. *Carcinogenesis* **14**:1633-1638.

Hein DW, Doll MA, Fretland AJ, Gray K, Deitz AC, Feng Y, Jiang W, Rustan TD, Satran SL and Wilkie TR Sr. (1997) Rodent models of the human acetylation polymorphism: comparisons of recombinant acetyltransferases. *Mutat Res* **376**:101-106.

Hein DW, Fretland AJ and Doll MA (2006) Effects of single nucleotide polymorphisms in human N-acetyltransferase 2 on metabolic activation (O-acetylation) of heterocyclic amine carcinogens. *Int J Cancer* **119**:1208-1211.

Kawamura A, Graham J, Mushtaq A, Tsiftsoglou SA, Vath GM, Hanna PE, Wagner CR and Sim E (2005) Eukaryotic arylamine N-acetyltransferase. Investigation of substrate specificity by high-throughput screening. *Biochem Pharmacol* **69**:347-359.

Kelly SL and Sim E (1994) Arylamine N-acetyltransferase in Balb/c mice: identification of a novel mouse isoenzyme by cloning and expression *in vitro*. *Biochem J* **302**:347-353.

Kent WJ (2002) BLAT--the BLAST-like alignment tool. *Genome Res* **12**:656-664.

Land SJ, Jones RF and King CM (1996) Genetic analysis of two rat acetyltransferases. *Carcinogenesis* **17**:1121-1126.

Leff MA, Epstein PN, Doll MA, Fretland AJ, Devanaboyina US, Rustan TD and Hein DW (1999) Prostate-specific human N-acetyltransferase 2 (NAT2) expression in the mouse. *J Pharmacol Exp Ther* **290**:182-187.

Lin SS, Yu CS, Wu JY, Tyan YS, Hsia TC, Lin WC and Chung JG (2005) Effects of aspirin on the in vitro and in vivo acetylation of 2-aminofluorene in Sprague-Dawley rats. *In Vivo* **19**:475-481.

Mushtaq A, Payton M and Sim E (2002) The COOH terminus of arylamine N-acetyltransferase from Salmonella typhimurium controls enzymic activity. *J Biol Chem* **277**:12175-12181.

Parker JM (1969) Human variability in the metabolism of sulfamethazine. *Hum Hered* **19**:402-409.

Patrianakos C and Hoffman D (1979) Chemical studies on tobacco smoke LXIV. On the analysis of aromatic amines in cigarette smoke. *J Anal Toxicol* **3**:150-154.

Rice P, Longden I and Bleasby A. (2000) EMBOSS: the European Molecular Biology Open Software Suite. *Trends Genet* **16**:276-277.

Rodrigues-Lima F, Delomenie C, Goodfellow GH, Grant DM and Dupret J (2001) Homology modeling and structural analysis of human arylamine N-acetyltransferase NAT1: evidence for the conservation of a cysteine protease catalytic domain and an active-site loop. *Biochem J* **356**:327-334.

Thomas MA, Chen CF, Jensen-Seaman MI, Tonellato PJ and Twigger SN (2003) Phylogenetics of rat inbred strains. *Mamm Genome* **14**:61-64.

Weber WW and Hein DW (1985) N-acetylation Pharmacogenetics. *Pharmacol Rev* **37**:25-27.

Wheeler DL, Barrett T, Benson DA, Bryant SH, Canese K, Church DM, DiCuccio M, Edgar R, Federhen S, Helmberg W, Kenton DL, Khovayko O, Lipman DJ, Madden TL, Maglott DR, Ostell J, Pontius JU, Pruitt KD, Schuler GD, Schriml LM, Sequeira E, Sherry ST, Sirotkin K, Starchenko G, Suzek TO, Tatusov R, Tatusova TA, Wagner L and Yaschenko E (2005) Database resources of the National Center for Biotechnology Information. *Nucleic Acids Res* **33**(Database Issue):D39-45.

Wick MJ and Hanna PE (1990) Bioactivation of N-arylhydroxamic acids by rat hepatic N-acetyltransferase. Detection of multiple enzyme forms by mechanism-based inactivation. *Biochem Pharmacol* **39**:991-1003.

Zhang X, Lambert JC, Doll MA, Walraven JM, Arteel GE and Hein DW (2006) 4,4'-methylenedianiline-induced hepatotoxicity is modified by N-acetyltransferase 2 (NAT2) acetylator polymorphism in the rat. *J Pharmacol Exp Ther* **316**:289-294.

FOOTNOTES

This work was partially supported by U.S. Public Health Service grant CA34627 from the National Cancer Institute and training grant ES011564 from the National Institute of Environmental Health Sciences. A preliminary report of this work was presented at the 95th Annual Meeting of the American Association for Cancer Research in Orlando, Florida, March 27-31, 2004. This work constitutes partial fulfillment by Jason Walraven for the Ph.D. in Pharmacology and Toxicology at the University of Louisville School of Medicine.

Send reprint requests to: David W. Hein, Ph.D., Department of Pharmacology and Toxicology, University of Louisville School of Medicine, Louisville, KY 40292. E-mail: d.hein@louisville.edu

FIGURE LEGENDS

Figure 1. Human, mouse, and rat N-acetyltransferase nucleotide (top) and amino acid (bottom) sequence comparisons (percent identical). Sequence comparisons were determined using EMBOSS pairwise alignment algorithms (Rice et al., 2000).

Figure 2. Western blot analysis of bacterial lysates using anti-Nat3 antiserum. The rat Nat3 selective antiserum identified rat Nat3 protein (~ 33.5 kDa) in lysates containing recombinantly expressed rat Nat3. No Nat band was visible in lanes of the negative control lysates (vector) or the lysates containing recombinantly expressed Nat1 or Nat2. Ponceau S red staining of the membrane was used as a loading control to verify equal protein loading in every lane.

Figure 3. Rat Nat1, Nat2, and Nat3 N-acetylation of various substrates. Activity is nmoles product per minute reaction time per mg total protein. Substrate concentrations were 300 μM (100 μM for MDA and MOCA). Error bars indicate standard error (n=3). Substrate abbreviations are defined in the methods section. Activity was not detected for substrates marked "ND." The scale of each graph differs depending on the activity of each isozyme. Rat Nat1 and Nat2 graphs have split y-axes to accommodate the wide range of activities.

Figure 4. Thermostability of rat N-acetyltransferases. Percent 2-aminofluorene N-acetyltransferase activity remaining plotted on the ordinate versus incubation time at 50^{o}C on the abscissa. Heat deactivation rate (k) and heat inactivation half-life ($T_{½}$) are indicated for each Nat isozyme.

Table 1

Rat N-acetyltransferase 3 PCR and sequencing primers.

Primer	Sequence	Features
Nat3-pf1	5'-GTAGCACCCGGGATGGACATTGAAGCGTACTT-3' [a]	*XmaI*, forward
Nat3-pr2	5'-ATGCGACTGCAGCTAAATAGTAAAAAAGCCAAT-3' [a]	*PstI*, reverse
Nat3-f1	5'-TCTTCTTTACTGGGCTCTGA-3'	forward
Nat3-f2	5'-TGCCATCTTCCACTTGACAGAA-3'	forward
Nat3-f3	5'-TGCATACTACCAGAAATCTCCAA-3'	forward
Nat3-r4	5'-CAGTAAAGAAGATGATTGACTTGAA-3'	reverse
Nat3-r5	5'-GTCAATTCCAGAGGCTCCCACAT-3'	reverse
Nat3-r6	5'-GATAAGAATGGTGCCTACTAAA-3'	reverse

[a] Restriction site underlined

JPET Fast Forward. Published on July 7, 2006 as DOI: 10.1124/jpet.106.108399
This article has not been copyedited and formatted. The final version may differ from this version.

Table 2

Apparent Michaelis-Menten kinetics and specificity constant for recombinant rat Nat1, Nat2, and Nat3.

	Apparent V_{max} (nmoles/min/mg)	Apparent K_m (μM)	Specificity Constant (nmoles/min/mg/μM)
AF			
Nat1	27.8 ± 1.9	37.0 ± 4.2	0.751
Nat2	644 ± 24	568 ± 44	1.13
Nat3	6.52 ± 0.08	33.1 ± 1.0	0.197
ABP			
Nat1	34.0 ± 1.8	5.83 ± 1.05	5.83
Nat2	706 ± 50	1570 ± 213	0.448
Nat3	4.33 ± 0.10	18.2 ± 1.6	0.238
N-hydroxy-ABP			
Nat1	0.633 ± 0.014	58.5 ± 2.0	0.0108
Nat2	2.03 ± 0.10	3300 ± 380	0.000615
Nat3	0.162 ± 0.007	62.0 ± 7.5	0.00262

JPET Fast Forward. Published on July 7, 2006 as DOI: 10.1124/jpet.106.108399
This article has not been copyedited and formatted. The final version may differ from this version.

Table 3

Comparisons of amino acid residues known to control substrate specificity.

Protein	Residue Number			
	125	129	127	280 – 290 [a]
Human NAT1	Phe	Tyr	Arg	VPKHGDRFFTI
Rat Nat2	Phe	Tyr	Arg	VPKHGDRFFTI
Mouse Nat2	Phe	Tyr	Arg	VPKHGDRFFTI
Human NAT2	Ser	Ser	Ser	VPKPGDGSLTI
Rat Nat1	Tyr	Tyr	Ser	VPKHGELVFTI
Mouse Nat1	Tyr	Tyr	Gly	VPKHGELVFTI
Rat Nat3	Phe	Cys	Phe	VPKCGNWLFTI
Mouse Nat3	Phe	Cys	Phe	VPKCGNVFFTI

[a] Differences within each group underlined

JPET Fast Forward. Published on July 7, 2006 as DOI: 10.1124/jpet.106.108399
This article has not been copyedited and formatted. The final version may differ from this version.

Human NAT2	87.4 81.0						
Rat Nat1	80.4 76.2	79.0 74.5					
Rat Nat2	84.0 81.4	80.3 73.8	84.9 82.8				
Rat Nat3	77.2 68.6	75.9 67.2	75.7 71.0	78.0 71.7			
Mouse Nat1	80.2 74.8	78.8 72.1	92.9 91.7	84.3 81.4	75.8 74.5		
Mouse Nat2	83.3 82.1	80.2 74.8	83.8 83.4	93.2 94.5	79.3 73.4	84.0 81.7	
Mouse Nat3	75.3 68.3	74.7 65.9	74.9 68.6	77.1 72.8	91.0 87.9	74.5 67.6	77.9 73.4
	Human NAT1	**Human NAT2**	**Rat Nat1**	**Rat Nat2**	**Rat Nat3**	**Mouse Nat1**	**Mouse Nat2**

Figure 1

JPET Fast Forward. Published on July 7, 2006 as DOI: 10.1124/jpet.106.108399
This article has not been copyedited and formatted. The final version may differ from this version.

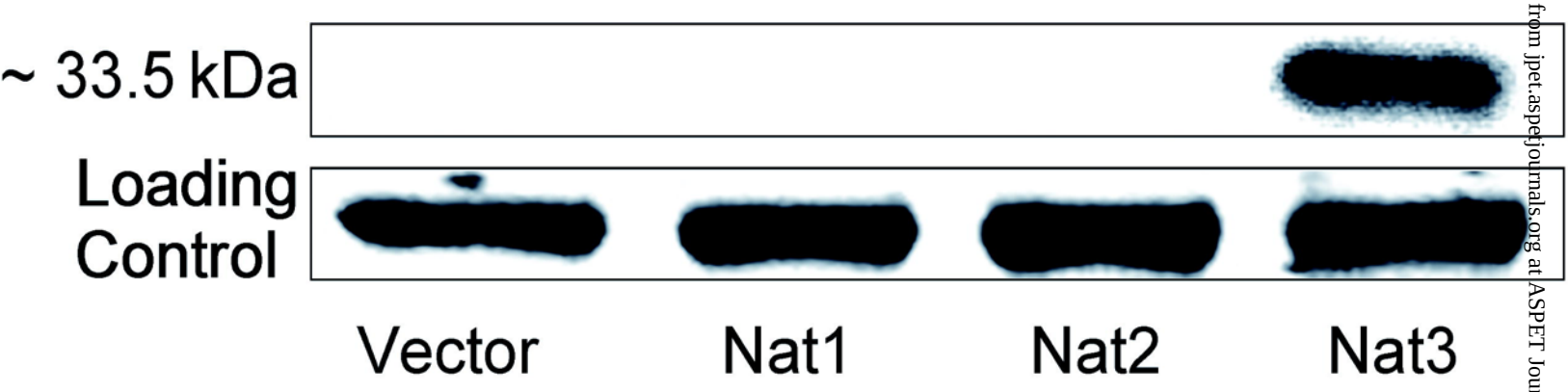

Figure 2

JPET Fast Forward. Published on July 7, 2006 as DOI: 10.1124/jpet.106.108399
This article has not been copyedited and formatted. The final version may differ from this version.

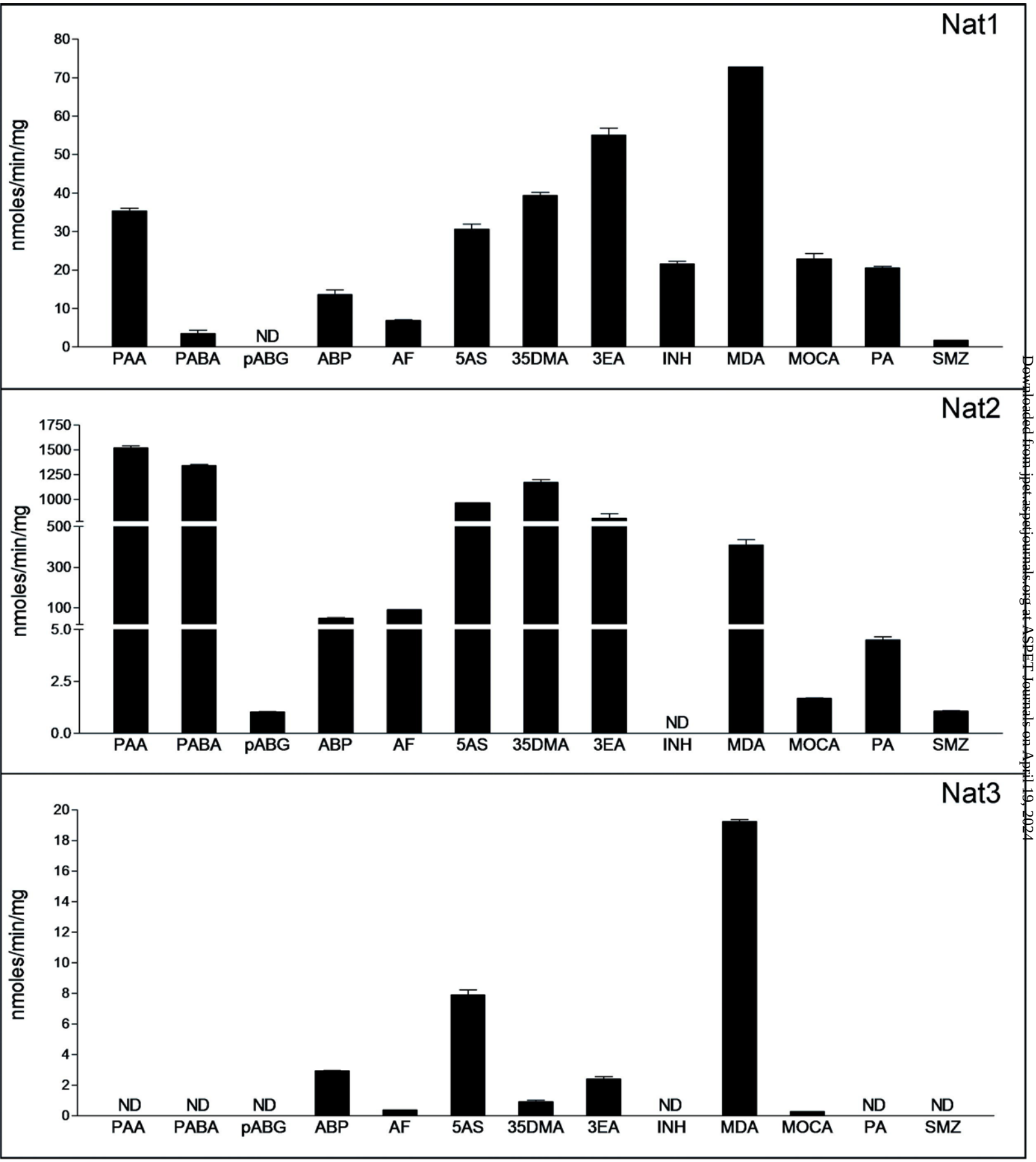

Figure 3

JPET Fast Forward. Published on July 7, 2006 as DOI: 10.1124/jpet.106.108399
This article has not been copyedited and formatted. The final version may differ from this version.

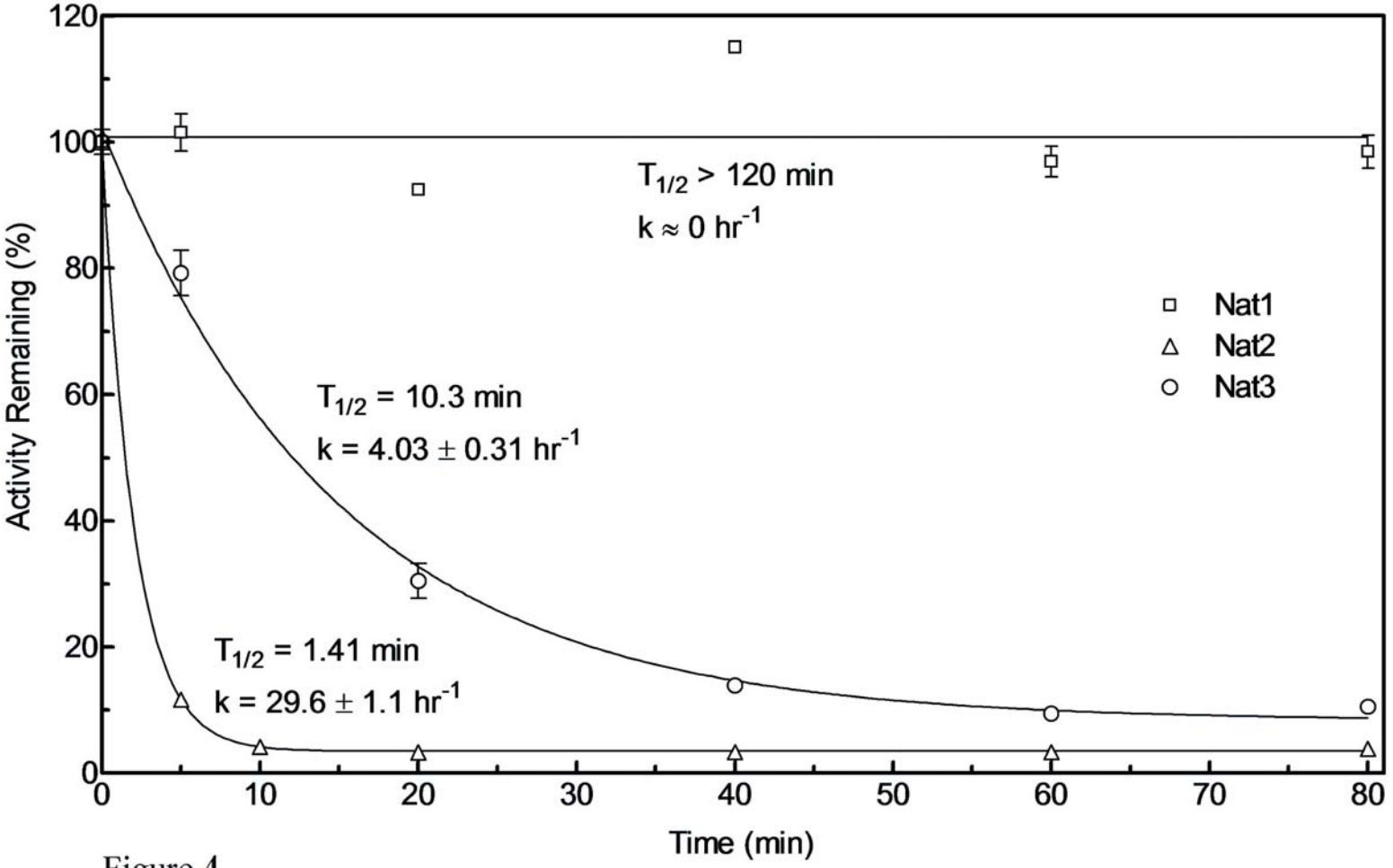

Figure 4